Published in final edited form as:
Eur J Neurosci. 2013 April ; 37(8): 1260–1269. doi:10.1111/ejn.12137.

GABAergic inhibition through synergistic astrocytic neuronal interaction transiently decreases vasopressin neuronal activity during hypoosmotic challenge

Yu-Feng Wang[1], **Min-Yu Sun**[2], **Qiuling Hou**[2,*], and **Kathryn A. Hamilton**[1]

[1]Department of Cellular Biology & Anatomy, Louisiana State University Health Sciences Center, Shreveport, LA, USA

[2]Department of Cell Biology & Neuroscience, University of California, Riverside, CA; USA

Abstract

The neuropeptide vasopressin is crucial to mammalian osmotic regulation. Local hypoosmotic challenge transiently decreases and then increases vasopressin secretion. To investigate mechanisms underlying this transient response, we examined effects of hypoosmotic challenge on the electrical activity of rat hypothalamic supraoptic nucleus (SON) vasopressin neurones using patch-clamp recordings. We found that 5 min exposure of hypothalamic slices to hypoosmotic solution transiently increased IPSC frequency and reduced firing rate of vasopressin neurones. Recovery occurred by 10 min exposure, even though the osmolality remained low. The $GABA_A$ receptor blocker, gabazine, blocked the IPSCs and the hypoosmotic suppression of firing. The gliotoxin l-aminoadipic acid blocked the increase in IPSC frequency at 5 min and the recovery of firing at 10 min, indicating astrocytic involvement in hypoosmotic modulation of vasopressin neuronal activity. Moreover, β-alanine, an osmolyte of astrocytes and GABA transporter inhibitor, blocked the increase in IPSC frequency at 5 min of hypoosmotic challenge. Confocal microscopy of immunostained SON sections revealed that astrocytes and magnocellular neurones both showed positive staining of vesicular GABA transporters (VGAT). Hypoosmotic stimulation *in vivo* reduced the number of VGAT-expressing neurones and increased co-localisation and molecular association of VGAT with glial fibrillary acidic protein that increased significantly by 10 min. By 30 min, neuronal VGAT labelling was partially restored and astrocytic VGAT was relocated to ventral portion while decreased in the somatic zone of the SON. Thus, synergistic astrocytic and neuronal GABAergic inhibition could ensure that vasopressin neurone firing is only transiently suppressed under hypoosmotic conditions.

Keywords

glia; hypothalamo-neurohypophyseal system; *in vitro* brainstem slice; neuroendocrinology; transporters

Introduction

Vasopressin is a nonapeptide synthesised by vasopressin neurones in several hypothalamic nuclei, including the supraoptic nucleus (SON) (Crowley & Armstrong, 1992; Caldwell *et*

Corresponding author: Yu-Feng Wang, Department of Cellular Biology and Anatomy, LSU Health Sciences Center-Shreveport, 1501 Kings Highway, Shreveport, LA 71103-4228, USA. Tel. +1-(318)-675-8326, Fax. +1-(318)-675-5889, ywang4@lsuhsc.edu.
*Current address: College of Animal Science and Technology, Shandong Agricultural University, Taian, Shandong, China.

The authors have no conflict of interest to declare

al., 2007). Vasopressin is essential for regulation of hydromineral balance. In response to hyperosmotic challenge, activity of vasopressin neurones increases and they release vasopressin into the bloodstream from their terminals in the posterior pituitary (Gainer *et al.*, 1977). Vasopressin neuronal activity is reduced in response to both brief *in vitro* (Richard & Bourque, 1995) and prolonged *in vivo* (Zhang *et al.*, 2001) hypoosmotic challenges. However, *in vitro* hypoosmotic challenge results in transient inhibition then recovery/rebound of vasopressin secretion in hypothalamic explants (Yagil & Sladek, 1990). These findings suggest that vasopressin-secreting system has the ability to adjust its sensitivity during hypoosmotic challenge. The mechanisms underlying this plasticity are not understood.

In hypothalamus, the SON is rich in synaptic innervations that can be detected in brain slices (Shibuya *et al.*, 2000) and their involvement in hypoosmotic modulation of vasopressin neuronal activity remain to be examined. On the other hand, astrocytes also play important roles in modulating osmotic responses (Hatton, 2004; Theodosis *et al.*, 2008). Retraction of astrocyte processes surrounding vasopressin neurones occurs in response to hyperosmotic challenge and is causally associated with increased firing activity of SON neurones and with increased vasopressin release. Within minutes of hypoosmotic challenge, SON astrocytes swell, then undergo a delayed regulatory volume decrease (RVD) (Hussy *et al.*, 2000), which is logically correlated with astrocytic process retraction. During RVD, astrocytes release β-alanine (Pasantes-Morales & Vazquez-Juarez, 2012), which inhibits GABA transporter (GAT) 3 that is mainly located on astrocytes and also on neurones in the SON (Park *et al.*, 2009). This astrocytic release of β-alanine should increase extracellular GABA levels and suppress vasopressin neuronal activity, theoretically. Nevertheless, it remains to be determined if hypoosmotic challenge inhibits vasopressin neuronal activity via changing GABAergic actions and if changes in astrocytic plasticity are temporally associated with GABAergic actions during this process. In addition, discrepancy between *in vitro* and *in vivo* data of hypoosmotic regulation remains to be interpreted with new evidence.

Here, we examine the time course of hypoosmolality-induced changes in vasopressin neurone firing and GABAergic synaptic transmission in male rat hypothalamic brain slices containing the SON. The results reveal for the first time that firing activity of SON neurones initially decreases and then recovers during hypoosmotic challenge, and that these changes are temporally-correlated with a transient increase then decrease in IPSC frequency. These hypoosmotic effects are blocked by disabling GABA transport. The results further show that both astrocytes and neurones express vesicular GABA transporter (VGAT) in the SON, expression of which is modulated by *in vivo* hypoosmotic challenge in synergy with changes in glial fibrillary acidic protein (GFAP), a major astrocyte cytoskeletal element. Together, our results indicate that increased GABAergic inhibition via temporally-correlated, intranuclear, glial-neuronal interactions dynamically modulate vasopressin neuronal firing in response to hypoosmotic challenge.

Materials and methods

Thirty-three 50–70 day-old male Sprague-Dawley rats (Harlan Labs, Placentia, CA and Prattville, AL, USA) were used. All animal procedures were in accordance with NIH and institutional guidelines, and approved by Institutional Animal Care and Use Committee of University of California, Riverside.

Patch-clamp recordings

Brain slice preparation and patch-clamp recording procedures were the same as those previously described (Wang & Hatton, 2007; Wang & Hatton, 2009). Animals were decapitated to minimise pain and discomfort. The brain was quickly dissected and then

immersed in oxygenated ice-cold normal aCSF (naCSF) for 1–2 min before being sectioned into 300 μm-thick coronal slices. The naCSF contained (in mM): 126 NaCl, 3 KCl, 1.3 $MgSO_4$, 2.4 $CaCl_2$, 1.3 NaH_2PO_4, 26 $NaHCO_3$, 10 Glucose, 0.2 ascorbic acid (305 mOsm/kg), adjusted to pH 7.4 with 2 MOPS (3-[N-morpholino] propanesulfonic acid) and bubbled with 95% O_2/5% CO_2. Chemicals were obtained from Sigma unless otherwise indicated. Slices were incubated in naCSF for ≥ 1 h at room temperature (21–23°C), then transferred to a recording chamber mounted on an upright microscope (Leica DM LFSA) and superfused with 35 °C naCSF or hypoosmotic aCSF (haCSF; 285 mOsm/kg, prepared by reducing NaCl of naCSF to 116 mM) at a speed of 1.2–1.5 ml/min. Somata of SON neurones were visually identified and membrane potential, action potential, and IPSCs were recorded in whole-cell configuration using an Axopatch 200B amplifier, 1320 digitiser (5 kHz sampling) and Clampex 10 software (Molecular Devices). Data collection began ≥10 min after achieving stable whole-cell configuration. The patch-pipette solution contained (in mM): 145 K-gluconate, 10 KCl, 1 $MgCl_2$, 10 HEPES, 1 EGTA, 0.01 $CaCl_2$, 2 Mg-ATP, 0.5 Na_2GTP, adjusted to pH 7.3 with KOH (295 mOsm/kg). For post-hoc identification of the chemical nature of recorded neurones, 0.5% Lucifer Yellow (K^+ salt) was routinely added to the pipette solution and the slices wherein recorded neurones failed to show phasic firing were subsequently immunostained for identification of vasopressin neurones. Membrane resistance and series resistance were also examined. Between successive tests slices were superfused with naCSF ≥ 15 min until recovery appeared.

Immunohistochemistry

We used immunohistochemical staining methods similar to those previously reported (Ponzio *et al.*, 2006; Wang & Hatton, 2009) to examine the distribution of GFAP and VGAT in the SON. The brain was removed and hypothalamic blocks containing the SON were immersed in ice-cold naCSF for 1–2 min before further processing. The two nuclei were randomly selected using for immunostaining or protein works. Blocks containing one SON were fixed in 4% paraformaldehyde in PBS (pH 7.4) for ~72 h at 4 °C and then sliced at 50 μm-thicknesses using a cryostat (Reichert-Jung). Supraoptic slices were permeabilised by incubation in PBS containing 0.3% Triton X-100 in PBS for 30 min at room temperature, then non-specific labelling was blocked by incubation for 1 h in 0.3% gelatine-containing PBS solution at room temperature. The slices were then incubated overnight at 4 °C in the gelatine-PBS containing a mixture of primary antisera (Santa Cruz Scientific, Inc., Santa Cruz, CA, USA) against GFAP (1:300, SC-33673), to identify astrocytes, and VGAT (1:300, SC-49574), to identify GABAergic cells. After washing, slices were incubated for 1.5 h at room temperature in gelatine-PBS containing secondary antisera labelled with Alexa Fluor® 488, 555 and/or 647 (1: 1000 dilution, Invitrogen, Carlsbad, CA, USA). Hoechst dye (0.5 μg/ml, 15min) was used to label nuclei. Non-specific labelling was excluded by neutralising primary antisera with blocking peptides and by eliminating primary or secondary antisera from the protocol. Sections were mounted in Vectashield (Vector Labs, Burlingame, CA, USA); fluorescence of Alexa Fluor® and Hoechst labelling was sequentially examined at 0.5 or 1 μm Z-axis intervals using a laser scanning confocal microscope (Leica TCP SP2). In the representative figures, single plane image was presented. In each animal, two to three slices from one SON were examined and averaged.

To verify the chemical nature of some of Lucifer Yellow-labelled neurones, methods similar to those stated above were used. After recording and Lucifer Yellow-labelling, the slice was fixed in 4% paraformaldehyde at 4°C overnight. After the permeabilisation and blockade, the slice was incubated in gelatine-PBS containing mouse anti-vasopressin-neurophysin (VP-NP, PS 41, gift from Dr. Gainer, NIH, 1:400) and goat anti-oxytocin neurophysin (SC-7810, 1:400). After washing, the slice was incubated for 1.5 h at room temperature in the gelatine-PBS containing a mixture of Alexa Fluor® 546- and 647-labeled secondary

antisera. Three-dimensional overlap of Lucifer Yellow-labelling with VP-NP labelling, in the absence of oxytocin neurophysin labelling, was used to identify vasopressin neurones (see Fig. 1) in the confocal microscopy.

Western blotting and Co-immunoprecipitation

The other SON from the same rats used for immunostaining was punched-out of hypothalamic tissue blocks and then lysed to obtain proteins for Western blotting and immunoprecipitation as previously described (Wang & Hatton, 2009). Briefly, SON lysates were centrifuged to remove insoluble components. The lysis buffer for Western blots contained: 50 mM Tris-HCl, pH 7.4; 150 mM NaCl; 0.1% (v/v) SDS; 50 mM NaF; 10 mM $Na_4P_2O_7$; 1 mM Na_3VO_4, 1% (v/v) Triton X-100 and 1 mM EGTA, and a cocktail of protease inhibitors (Halt Protease Inhibitor Cocktail, Thermo Scientific). For co-immunoprecipitation, Triton X-100 and EGTA were replaced with 1% (v/v) NP-40 and 1 mM EDTA. Concentration of soluble proteins was assayed using the BCA protein assay reagent (Thermo Scientific Pierce, Rockford, IL, USA). For Western blotting of GFAP, 60 μg of protein per lane was separated on a 10% SDS-PAGE gel and then transferred onto a polyvinylidene difluoride (PVDF) membrane (Millipore, Billerica, MA, USA). For co-immunoprecipitation, total lysates were pre-cleared with protein A agarose (Millipore), and then 1.0–1.5 mg of protein obtained from the SON lysate was incubated with 1.5 μg of immunoprecipitating antibody against GFAP to form immune complexes. After overnight incubation at 4°C, the immune complex was captured by adding 50 μl of protein A agarose bead slurry through gently rocking for 2 h at 4°C. The agarose beads were then collected by a pulse centrifugation. After discarding the supernatant and washing the beads, the protein-loaded beads were re-suspended in sample buffer and boiled for 10 min. The beads were then spun down, and the supernatant was separated on a 10% SDS-PAGE gel and then transferred onto a PVDF membrane at 4°C. The membrane was probed with antibodies against GFAP (1:300 dilution), actin (Cat. No. SC-1616, 1 :500) or VGAT (1:300 dilution) for 4 h after pre-treatment with 5% dry milk (w/v in PBS) for 1 h at room temperature. For reprobing, membranes were stripped off preceding antibodies. Protein immunoblotting bands were visualised using horseradish peroxidase-conjugated secondary antibodies and an enhanced chemiluminescence detection system. Positive and negative controls consisted of total lysates and non-specific IgG, respectively. All reagents for immunoblotting detection were from GE Healthcare (Little Chalfont, Buckinghamshire, UK)

Data collection and analysis

Patch-clamp recordings, confocal images and protein bands were analyzed as previously described (Wang & Hatton, 2009). In brief, if a neurone exhibited phasic firing pattern or positive immunostaining for VP-NP, it was considered to be a vasopressin neurone. We quantified membrane potential, firing frequency, IPSC frequency and IPSC amplitude 0–2 min before, 4–6 min and 9–11 min after starting superfusion of hypoosmotic solution. We identified IPSCs as brief (10–100 msec) outward currents at a holding potential of −10 mV; this identification was further verified by blockade of this postsynaptic current with 10 μM gabazine. Voltage measurements were not corrected for the liquid junction potential (−8 to −11 mV).

To distinguish neurones from astrocytes in analysing immunostaining, we also used Hoechst to stain nuclei. Astrocytes had the homogeneously stained small, round, or elliptical nuclei and magnocellular neurones had non-homogeneously-stained larger (> 8μm), round, nuclei (Paterson & Leblond, 1977). To quantify immunoreactivity of SON neurones and astrocytes the background fluorescence of each fluorophore was set at 1 of 256 grey levels during scanning and corrected using minimum baseline correction function (Leica LCS Lite software) during analysis. The intensity of each label was then calculated relative to the

background intensity. To evaluate VGAT labelling associated with GFAP filaments, images of filaments longer than 5 μm were collected using a 63× objective. A 4×4 grid was overlaid on the images, the average intensity of three randomly-selected boxes was determined, and the ratio of VGAT to GFAP labelling was calculated. In counting the number of VGAT positive neurones, the soma around magnocellular nucleus was counted in low magnification, which should have a minimal 20% greater intensity above the background staining. Actin was used as the loading control in quantifying GFAP expression. In co-immunoprecipitation, target protein levels were determined using their relative amount to the immunoprecipitated proteins in corresponding lanes.

Statistical analyses were performed using Student's paired t-test (two group data, two tails) and one way repeated measures Analysis of Variance (ANOVA, for data ≥ three group) using SigmaPlot 11 software (Systat Software, Inc., San Jose, CA, USA). In pair comparison with Wilcoxon Signed Rank Test, significant level was set at $P = 0.05$. In all Pairwise Multiple Comparison Procedures (ANOVA on Ranks, Tukey Test or Chi-Square Test), $P < 0.05$ was considered significant. In all Pairwise Multiple Comparison Procedures (Holm-Sidak method), significant levels were set at 0.05, 0.025 and 0.017 for comparisons of control versus 5 min (the first order), 5 min versus 10 min (the second order) and control versus 10 min (the third order), respectively. Data are presented as mean ± SEM of raw or normalised (percent) values.

Results

In this study, 16 rats were used for patch clamp recording and 17 rats were used for immunohistochemical staining, Western blotting and immunoprecipitation.

Hypoosmotic challenge transiently decreases firing rate and increases IPSC frequency of vasopressin neurones

Whole-cell patch clamp recordings were obtained from 48 putative vasopressin neurones in SON slices superfused with naCSF (305 mOsm/kg) and then with haCSF (285 mOsm/kg). Of the 48 neurones, 40 exhibited phasic firing, typical feature of vasopressin neurones. The eight non-phasic firing cells were also identified to be vasopressin neurones by immunohistochemical staining for VP-NP. Other cells that were not identified electrophysiologically or immunohistologically were not included in the analysis to avoid confusion due to potential difference of different neuronal types, i.e., vasopressin versus oxytocin neurones. The resting membrane resistance in naCSF was 391.0 ± 58.1 MΩ ($n = 7$), which was a stable value measured 10–15 min after gradually deceasing from a relatively high level (480–1040 MΩ) at the beginning of whole-cell configuration and similar to those reported previously (Muller *et al.*, 1999; Wang & Hatton, 2004). The series resistance was 24.4 ± 2.5 MΩ in naCSF and unchanged after 10 min in haCSF (23.4 ± 2.5 MΩ; $n = 7$, $P > 0.05$).

Firing activity of nine vasopressin neurones from three rats was recorded in current-clamp mode. Nine of the neurones exhibited phasic firing and three exhibited non-phasic firing but VP-NP-immunoreactivity. The hypoosmotic challenge significantly changed the firing rate (ANOVA on Ranks, Chi-square =17.261 with 2 degrees of freedom, $P < 0.001$ by Tukey Test) and the basal membrane potential ($F = 11.212$, $P < 0.001$ by Holm-Sidak method). A recording from a putative vasopressin neurone is shown in Figure 1Aa with immunostaining in Figure 1Ab, and a summary graph for all 12 cells is shown in Figure 1Ac. After 5 min in haCSF, the firing rate of the 12 neurones was ~41% lower than it was in naCSF (3.41 ± 0.85 Hz in naCSF, 2.01 ± 0.61 Hz in haCSF, $q = 4.907$, $P < 0.05$), and the membrane potential was also hyperpolarised (−54.9 ± 1.8 mV in naCSF, −58.3 ± 2.7 mV in haCSF, $t = 2.688$, $P = 0.013$, Figure 1Ab2). After 10 min superfusion with haCSF, however, the firing rate was

significantly higher (4.87 ± 1.53 Hz) than it was at 5 min (q = 5.052, P <0.05) and the membrane potential (−52.3 ± 2.4 mV) was relatively depolarised compared to that at 5 min (t =4.72, P <0.001). Despite dramatic difference in the average firing rate between those at 10 min and control, the higher variability after hypoosmotic challenge made this difference insignificant (q =0.144, P >0.05). At 15 min washout with naCSF, the firing rate was 2.31 ± 1.01 Hz, which did not differ from the initial firing rate in naCSF (P =0.240) while the membrane potential remained at a relatively depolarised state (−52.7 ± 2.4 mV). In the analysis, we have also tried to look into the intra-burst frequency of the phasic firing (Bull *et al.*, 2006) and identified a trend of reduction and then increase in the intraburst frequency in parallel with the initial inhibition and later excitation, respectively. However, different from hyperosmotic stimulation, the initially dramatic suppression or the later rebound increase in the firing rate made the “phasic” discharges obscured; thus, we could not present this result statistically.

Vasopressin neurones receive synaptic inputs from GABAergic neurones located in and around the SON (Sladek & Armstrong, 1987), the suprachiasmatic nucleus (Cui *et al.*, 1997), and arcuate nucleus (Ludwig & Leng, 2000). In slices, the initial inhibitory effect of haCSF on vasopressin neurone firing could therefore result from increased synaptic inhibition from GABAergic neurones in the SON or its vicinity. To examine potential involvement of inhibitory synaptic inputs in the response to hypoosmotic challenge, in four rats we recorded IPSCs of 7 phasic firing neurones and 5 non-phasic neurones that were VP-NP immunopositive. The hypoosmotic challenge significantly changed IPSCs frequency (ANOVA on Ranks, Chi-square =12.167 with 2 degrees of freedom, P =0.002 by Tukey Test) although IPSC amplitude was not significantly affected (Chi-square =0.298 with 2 degrees of freedom, P =0.862; Fig. 1Bb). As shown in Figure 1B, after 5 min in haCSF the IPSC frequency was 5.4 ± 1.6 Hz, which was significantly higher than it was in naCSF (2.8 ± 0.9 Hz, q =4.907, P <0.05). Noteworthy was the occurrence of outward current around the peak increase in IPSC frequency, which ranged from 5 pA to 40 pA. After 10 min, the IPSC frequency was lower than the frequency at 5 min (4.8 ± 1.6 Hz, q =2.887, P >0.05), and it did not differ from the frequency in naCSF (q =2.021, P >0.05). After 15 min wash in naCSF, the IPSC frequency was 4.0 ± 1.5 Hz, which was further lower than the frequency at 5 min in haCSF (P =0.381).

Hypoosmolality-induced transient suppression is mediated by GABAergic inhibition

IPSCs are generally considered to be GABAergic. Thus, changes in extracellular GABA levels at synapses could underlie the transient inhibitory effect of haCSF on IPSCs. However, hypoosmotic challenges also trigger astrocytic release of taurine, an inhibitory osmolyte (Pasantes-Morales *et al.*, 1993), which can activate glycine receptors (Hussy *et al.*, 2000), thereby increasing non-GABAergic IPSCs and tonic outward currents (Ghavanini *et al.*, 2006). To distinguish between these possibilities, we tested whether the IPSCs observed during c effects of haCSF on firing activity of five vasopressin neurones from two rats in the presence of gabazine (10 μM, 10 min), which blocks $GABA_A$ receptors. The result showed that gabazine reversed the transient inhibition of the hypoosmotic stimulation on the firing activity (ANOVA on Ranks, with percentage standardisation, Chi-square =8.400 with 2 degrees of freedom, P =0.008). As shown in Figure 2A and 2B, the firing rate after 10 min in naCSF + gabazine was 2.2 ± 0.8 Hz, which did not differ significantly from the basal firing rate in naCSF alone (1.2 ± 0.6 Hz, q =2.683, P >0.05). However, after 5 min in haCSF + gabazine, the firing rate was 3.3 ± 1.2 Hz, significantly higher (q =4.025, P <0.05 versus naCSF + gabazine), and it remained at higher levels at 10 min relative to haCSF + gabazine (3.6 ± 0.9 Hz, q =2.683, P >0.05). In these five neurones, IPSCs as well as the tonic outward currents were completely blocked by the presence of gabazine for 5–10 min (Fig. 2C), supporting their GABAergic nature. These results are consistent with a previous report

(Sladek & Armstrong, 1987) that $GABA_A$ receptor antagonists stimulated vasopressin release in a concentration-dependent manner in hypothalamo-neurohypophyseal explants. It indicates that $GABA_A$ receptor-mediated IPSC plays an essential role in the hypoosmolality-induced inhibition of vasopressin neuronal firing activity.

Astrocytic GABA transport affects vasopressin neuronal activity during hypoosmotic challenge

As mentioned above, hypoosmotic challenge could result in astrocytic swelling and RVD, which would be expected to affect firing activity of vasopressin neurones. To examine this possibility, we used a gliotoxin, l-aminoadipic acid (L-AAA, Sigma, Cat. No. A7275), to disable astrocytic functions as in previous studies (Wang & Hatton, 2009). Brain slices superfused with naCSF containing L-AAA (0.25 mM) did not significantly change the firing rate (1.2 ± 0.3 Hz in naCSF versus 1.3 ± 0.6 Hz in L-AAA for 15 min, $n = 9$, Z = −0.059, $P = 1.0$ by Wilcoxon Signed Rank Test) in slices from two rats. In six cells, further superfusion of the slices with haCSF in the presence of L-AAA did not significantly change the firing rate (ANOVA on Ranks, Chi-square =1.652 with 2 degrees of freedom, $n = 6$, $P = 0.430$). As shown in Figure 3A1, just before haCSF in the presence of L-AAA, the firing rate of vasopressin neurones was 0.51 ± 0.20 Hz, which did not differ significantly from the firing rate after 5 min in haCSF + L-AAA (0.29 ± 0.12 Hz) or after 10 min in haCSF + L-AAA (0.29 ± 0.13 Hz), suggesting a reduction of inhibition and blockade of the recovery of firing rate. In addition, the resting membrane potential did not differ (−52.3 ± 1.2 mV in naCSF + L-AAA; −54.2 ± 1.6 mV after 5 min haCSF + L-AAA; −54.2 ± 2.2 mV after 10 min haCSF + L-AAA, $F = 0.27$, $P = 0.769$; Fig. 3B). The absence of haCSF effects, particularly the trend of recovery from the inhibition in the presence of L-AAA, suggest that astrocytic functional plasticity plays a role in the recovery of vasopressin neuronal firing in response to hypoosmotic challenge.

One approach of astrocyte modulation of GABAergic actions is through GABA transport in the SON (Park *et al.*, 2006). If the action of L-AAA involved astrocytic GABA transport as suggested by a previous study (Park *et al.*, 2009), then L-AAA might also affect IPSC frequency or tonic inhibitory/outward currents by inhibiting GATs in the SON (Park *et al.*, 2009). This possibility was further tested. As shown in Figure 4A, brain slices from two rats superfused with naCSF containing L-AAA did not significantly change IPSC frequency (1.9 ± 0.6 Hz in naCSF versus 2.9 ± 1.6 Hz in naCSF + L-AAA, $t = -0.639$ with 5 degrees of freedom, $n = 6$, $P = 0.551$). In response to haCSF, the IPSC frequency (2.9 Hz ±1.6 Hz in naCSF + L-AAA) reduced to 1.2 ± 0.4 Hz after 5 min and to 1.1 ± 0.5 Hz after 10 min in haCSF + L-AAA. The IPSC frequency therefore appeared to be lower in haCSF than in naCSF, but the difference was not significant (ANOVA on Ranks, Chi-square= 6.661 with 3 degrees of freedom, $n = 6$, $P = 0.084$; Fig. 4Ab). It is worth of stressing that relative to the IPSC frequency in naCSF + L-AAA, the IPSC frequency was not higher in haCSF + L-AAA at 5 min. These results therefore support involvement of astrocytic GABA transport activity in mediating effects on hypoosmotic challenge on vasopressin neurone firing activity.

In the SON, as in other brain regions, GATs play an important role in regulating extracellular GABA levels (Voisin *et al.*, 1994), and L-AAA possibly inhibits GAT activity (Park *et al.*, 2009). However, L-AAA can have other effects, such as on glutamate transport (Colombo, 2005). To confirm the role of GATs in vasopressin neuronal responses to hypoosmotic challenge, we therefore examined effects of GAT inhibition on IPSC frequency. We tested effects of β-alanine (150 μM, Sigma, Cat. No. 05159), an osmolyte of astrocytes (Pasantes-Morales & Vazquez-Juarez, 2012) and GAT 3 inhibitor (Park *et al.*, 2009), on IPSC frequency in brain slices from two rats. The result showed that pre-treatment with β-alanine blocked the transient increase of IPSC frequency at 5 min of the hypoosmotic stimulation (ANOVA on Ranks, Chi-square= 1.652 with 2 degrees of freedom, $n = 6$, P

=0.430). As shown in Figure 4B, the IPSC frequency in naCSF + β-alanine was 1.1 ± 0.4 Hz, which did not differ from the frequency after 5 or 10 min in haCSF + β-alanine (0.8 ± 0.3 Hz after 5 min, 0.9 ± 0.3 Hz after 10 min). These results support a role for GABA reuptake, most likely by astrocytes, in suppression of vasopressin neurone firing during hypoosmotic challenge.

Hypoosmolality modifies VGAT expression in both SON astrocytes and neurones

The results above indicate that GABA uptake and the associated GABAergic inhibition regulate responses of vasopressin neurones to hypoosmotic challenge. To identify the source of local GABAergic modulation of vasopressin neurone activity in the SON, we examined immunoreactivity of the SON for VGAT, a marker for GABAergic synaptic vesicles, as well as for GFAP, to identify astrocytes. Then, we observed responses of VGAT and GFAP to *in vivo* hypoosmotic challenges.

In these experiments, we first examined time-associated plasma osmolality, i.e., 0 min (control, immediately), 10 min and 30 min after intraperitoneal H_2O administration (20 ml/kg body weight). The result showed that this *in vivo* hypoosmotic challenge time-dependently reduced plasma osmolality: 297.1 ± 1.1 mOsm/kg at 0 min, 285.3 ± 0.6 mOsm/kg at 10 min and 279.2 ± 1.9 mOsm/kg at 30 min ($n = 6$, $F = 4.252$, $P = 0.046$). The result showed that hypoosmotic challenge significantly reduced rat plasma osmolality but the rate of osmotic change was obviously slow. In accordance with the finding that hypoosmotic effect *in vitro* is of rate-dependent actions (Yagil & Sladek, 1990), the slower building of hypoosmotic levels *in vivo* predisposes a slower onset of *in vivo* hypoosmotic effects.

With this finding in mind, we performed co-immunostaining of GFAP with VGAT at three time points (0 min, 10 min and 30 min) with five rats in each group after determining the peak reactions of VGAT and GFAP in preliminary trials. As shown in Figure 5Aa, VGAT immunostaining overlapped with GFAP immunostaining of astrocytic processes surrounding magnocellular neurone somata. In the merged image, the arrow points to an astrocytic process that expressed both VGAT and GFAP. Moreover, GFAP-negative neuronal somata (arrowhead) were also VGAT positive. This pattern of immunostaining was observed in SON slices from all 15 rats. In contrast, the control sections without primary (i.e., VGAT) or secondary antibodies did not show any specific staining (Fig. 5Ab1 and b2). Thus, both SON astrocytes and magnocellular neurones could be the local sources of GABAergic inhibition of vasopressin neurones in hypothalamic slices.

In response to hypoosmotic stimulation in three rats, the ratio of VGAT-positive GFAP filament in astrocyte processes changed significantly in three rats ($n = 3$, each averaged from three randomly-selected areas, $F = 212.9$, $P < 0.001$). Compared to controls (100%), the ratio of VGAT-positive GFAP filament were significantly high at 10 min (132.6 ± 5.8 %, $t = 7.699$, $P = 0.002$) and significantly low at 30 min (47.1 ± 2.0 %, $t = 12.728$, $P < 0.001$; Fig. 5Bab, the second columns). In whole SON, however, VGAT intensity did not change significantly (88.0 ± 4.1 % of control at 10 min and 116.3 ± 4.1 of control at 30 min, $F = 5.546$, $P = 0.07$). This trend of bidirectional change was associated with the changes in the number of VGAT-positive neurones ($F = 25.526$, $P = 0.005$). At 10 min, the number of VGAT-positive somata was 40.2 ± 7.7% of control ($t = 7.133$, $P = 0.002$) and at 30 min, the number recovered to 67.0 ± 11.0% of control, which is significantly higher than that at 10 min ($t = 3.025$, $P = 0.033$). At 30 min, transiently increased GFAP at 10 min dropped to control levels.

During this hypoosmotic challenge, VGAT staining at the ventral glial lamina where the astrocyte somata are located increased gradually: 133.9 ± 7.8 % of control at 10 min ($n = 3$, $t = 3.686$, $P = 0.021$) and 193.7 17.6 % of control at 30 min ($t = 10.511$, $P < 0.001$ to control and

t =6.825, P =0.002 to 10 min). Figure 5B shows representative images in low (Fig 5. Ba) and high (Fig 5. Bb) magnifications.

The immunofluorescent staining shows that GFAP increases transiently in response to hypoosmotic challenge. This change is further validated by Western blotting assays of GFAP levels throughout the *in vivo* hypoosmotic challenge (n =4, F =6.679, P =0.03). As shown in Figure 5C, the GFAP level increased within 10 min of hypoosmotic challenge (136.5 ± 3.5 % of control, n =4, t =3.356, P =0.012). By 30 min, however, the level did not differ from the control level (110.9 ± 9.5 % of control, t =1.066, P =0.327). This result temporally matches the transient increase in GFAP filament and is consistent with the reduction in the firing rate of VP neurones.

To establish an association of *in vivo* findings with *in vitro* results and to test the influence of rate-dependent hypoosmotic actions (Yagil & Sladek, 1990), we used GFAP as a marker to test *in vitro* effect of haCSF on astrocytic plasticity in brain slices from three rats. Similar to the *in vivo* findings, treatment of the slices with the haCSF significantly increased the levels of GFAP (138.6 ± 3.9% of control, $p<0.05$) at an earlier time point (5 min) while at 20 min of the hypoosmotic challenge GFAP intensity (94.4 ± 12.5% of control, n = 5, P >0.05) returned to control levels just prior to the stimulation. Compared to our *in vivo* results and astrocyte cultures (Pasantes-Morales & Vazquez-Juarez, 2012), the different time courses to the peak support the view that hypoosmotic actions are rate-dependent (Yagil & Sladek, 1990).

Molecular association between GFAP and VGAT

With plastic changes in GFAP expression, the initial VGAT increase in GFAP-positive astrocytic processes possibly reflects an expansion/elongation of GFAP filaments and their associated VGAT; the later reduction of VGAT in the somatic zone (middle and dorsal portion of the SON) reflects a collapse of GFAP and dispersion/translocation of its associated VGAT. This relationship well matches the guiding role of GFAP in distribution of other astrocytic proteins that we previously proposed (Wang & Hamilton, 2009); however, this possibility remains to be examined in hypoosmotic regulation of vasopressin neuronal activity. Based on the VGAT immunostaining results, we further hypothesised that VGAT is molecularly associated with GFAP, and the extent of this association can be altered during hypoosmotic challenge. To test this hypothesis, we performed co-immunoprecipitation experiments to examine interactions between GFAP and VGAT in the SON lysates dissected at 0 min, 10 min and 30 min after hypoosmotic challenge. As shown in Figure 5D, the molecular association between GFAP and VGAT was increased significantly at 10 min (n = 3, P <0.05), which fell back to the control levels at 30 min of the challenge. This change is consistent with the morphological findings and supports our hypothesis.

Discussion

This study provides electrophysiological evidence that inhibitory GABAergic currents modulate vasopressin neuronal firing during hypoosmotic challenge. The response is transient, however. An initial, transient, decrease in vasopressin neuronal firing occurs, which is possibly mediated by increased GABAergic inhibition partially due to β-alanine-mediated reduction of GABA uptake in astrocytes. The subsequent recovery of firing occurs possibly due to a decrease in GABAergic inhibition, a result of increased GABA uptake, particularly in neurones. Thus, there is a synergistic interaction between astrocytes and neurones in the transient GABAergic inhibition of vasopressin neuronal activity during hypoosmotic challenge.

Dual effect of hypoosmolality on vasopressin neuronal activity

Hypoosmotic challenge of the SON in brain slices evoked an initial inhibition and subsequent recovery of vasopressin neurone firing activity. This finding is consistent with the report that hypoosmotic stimulation initially decreased and then increased vasopressin release in rat hypothalamic explants (Yagil & Sladek, 1990). The initial inhibition of vasopressin neuronal activity is also consistent with the increased IPSC frequency as well as previously observed inhibitory effects of acute hypoosmotic challenge on vasopressin neuronal activity (Richard & Bourque, 1995; Kusano *et al.*, 1999). The subsequent reduction of IPSC frequency and membrane depolarisation are in agreement with the recovery of vasopressin neuronal discharges. The transient nature of the response to hypoosmotic challenge supports our view that relative reduction in osmolality can cause adaptive changes in the osmosensory threshold of vasopressin neurones (Wang *et al.*, 2011).

What needs to be addressed here is the time course of the inhibitory phase and the differences between *in vivo* and *in vitro* observations. In the hypothalamic explants (Yagil & Sladek, 1990), the inhibition of vasopressin release peaks between 20 min and 60 min whereas, the decrease in spiking and increase in IPSCs in this study peak at 5 min and recover by 10 min. This discrepancy is obviously associated with the dependency of osmotic effects on the rate of osmotic change (Yagil & Sladek, 1990) and on the nature of assay methods. Apparently, changes in osmolality occur quicker on a cell or cellular groups on the surface of brain slices than that inside of the thick hypothalamic explants. The later condition requires more time for osmolytes to evoke a measurable accumulation of vasopressin in extracellular medium compared to changes in cellular electrical activity detected by patch-clamp recording. For the same reason, haCSF-evoked expression of GFAP in brain slices was quicker than the change in the brain *in vivo* but much slower than those in cell cultures (Hussy *et al.*, 2000). Therefore, despite the apparent differences in their time course, the basic cellular processes should be the same in nature between these different observations.

Lastly, factors underlying differences between the transient *in vitro* inhibitory effects and prolonged *in vivo* suppressive effects (Zhang *et al.*, 2001) need to be considered. The first factor is taurine. It has been reported that GABA-activated currents *in vitro* were not antagonised by strychnine, a blocker of glycine/taurine receptor; however, locally applied strychnine increased basal electrical activity of vasopressin neurones *in vivo*, particularly during hypoosmotic stimulation (Hussy *et al.*, 1997). In brain slices, effects of taurine were minor if any, which might be due to its being rapidly exhausted during longer incubation of the slices *in vitro* (Miyata *et al.*, 1997). However, taurine loss is slower in the brain (Verbalis, 2010). This difference in taurine metabolism *in vivo* versus *in vitro* could partially account for the persistent inhibition of vasopressin neurones in the hypoosmotic rat model (Zhang *et al.*, 2001) and transient inhibition in hypothalamic explants (Yagil & Sladek, 1990) and in the brain slices. Other possibilities may involve different glutamatergic innervations and function-associated shifts of Cl^- reversal potential, etc. About the later possibility, it has been reported that prolonged dehydration could turn inhibitory GABAergic action to excitatory effect on vasopressin neurones due to positively shifting Cl^- reversal potential (Kim *et al.*, 2011). Alternatively, under certain circumstances, the GABA reversal potential could be more positive than the resting membrane potential in vasopressin neurones (Haam *et al.*, 2012). Thus, if prolonged hypoosmotic challenge negatively shifts the Cl^- reversal potential, as opposite machinery to the hyperosmotic actions, the *in vitro* rebound/recovery from transiently inhibitory effects may be masked *in vivo*.

Inhibitory synaptic inputs on vasopressin neuronal activity

Synaptic transmission plays a critical role in osmotic modulation of vasopressin neuronal activity, particularly glutamatergic inputs (Brown *et al.*, 2004; Israel *et al.*, 2010). Thus, in our preliminary study, we have first observed hypoosmotic effects on EPSCs. Unexpectedly, we found a delayed decrease but not a dramatic increase in EPSC frequency when the recovery of firing rate occurred. Although, this could imply that external excitatory inputs play a critical role in the neuronal modulation from anterior peri-third ventricular structures and other osmosensitive areas (Leng *et al.*, 1989; Honda *et al.*, 1989), we have no evidence to link the transient suppression of vasopressin neuronal activity with rapid changes in glutamate release in the SON that has been found at cell cultures (Pasantes-Morales *et al.*, 1993).

In contrast to the delayed, “irrelevant”, change in EPSCs, robust alteration in IPSC frequency was observed. IPSCs of the SON neurones are classically considered to originate from GABAergic synapses from interneurones located at numerous brain loci around the SON (Randle *et al.*, 1986; Sladek & Armstrong, 1987; Cui *et al.*, 1997; Ludwig & Leng, 2000). The present results show that hypoosmolality-induced GABAergic inhibition of vasopressin neurones occurs in the absence of most external GABAergic inputs in the hypothalamic slice. Additionally, innervations of the perinuclear zone of SON neurones are rare (Armstrong & Stern, 1997). These facts suggest the presence of intranuclear GABAergic cells in the SON, which is verified in this study by presence of and coordinated changes in VGAT expression in the SON. Together with the early finding (Sladek & Armstrong, 1987) in hypothalamo-neurohypophyseal explants, even without measuring Cl^- reversal potential directly, we can still conclude that GABAergic cells within the SON exert an autoinhibitory effect on vasopressin neuronal activity.

Astrocytic-vasopressin neuronal interaction in GABAergic actions during hypoosmotic challenge

Astrocytic involvement is clear as demonstrated by the presence of tonic GABA current, L-AAA blockade of the depression, and dual change in the expression of VGAT and GFAP. Meanwhile, changes in IPSC frequency and VGAT expression strongly suggest neuronal participation. Thus, the transient effect possibly results from coordinated responses of astrocytes and vasopressin neurones to hypoosmotic challenge.

Astrocytes can extensively influence vasopressin neuronal activity (Hatton, 2004; Theodosis *et al.*, 2008) and this influence is again highlighted in the present study. The blockade of the transient response of vasopressin neurones to hypoosmotic challenge by L-AAA and β-alanine suggests that astrocytic GATs play an active role in regulating extracellular GABA. Our immunohistochemical staining results show that astrocytic processes surrounding vasopressin neuronal somata contain VGAT, which indicates the ability of astrocytes to release and to pack GABA in vesicles. It is possible that the release of β-alanine during RVD (Pasantes-Morales *et al.*, 1993) inhibits GATs and increases extracellular GABA levels (Voisin *et al.*, 1994), which could account for the tonic outward current accompanying with the increased IPSC frequency (Park *et al.*, 2009). The increased association between GFAP and VGAT at the early stage of hypoosmotic stimulation, which mainly occurred in astrocyte processes around vasopressin neurones, highlights that an increased availability of GABAergic synaptic vesicles is ready to pack newly retrieved GABA once GATs become active. There is also possible GABA release from astrocytes via permeation through the Bestrophin 1 anion channel as seen in the cerebellum (Lee *et al.*, 2010). A potential GABA release from astrocytes could occur simultaneously with β-alanine inhibition of GATs, accounting for tonic outward currents. Noteworthy is that β-alanine sensitive GAT 3 is also expressed by SON neurones (Park *et al.*, 2009). Thus, vasopressin

neurones could also be the target of β-alanine and inhibition of neuronal GAT 3 at the early stage can contribute to the transient increase in IPSCs and decrease in firing activity. Relative to the extrasynaptic GABA actions, GABA release from SON neurones at the early stage should be a dominant source of increased IPSC frequency because of the dramatic reduction of neuronal VGAT, a result of increased GABA release and reduced uptake.

As RVD progresses, however, astrocytic β-alanine would be exhausted (Pasantes-Morales *et al.*, 1993) and restored GAT activity would ensure that extracellular GABA decreases, resulting in recovery of vasopressin neurone firing, partially because of increased GABA uptake and transport of VGAT from astrocyte processes to the ventral glial lamina. This is evidenced by the recovery of the outward currents and VGAT images. As neuronal GABA release reduction and/or GABA uptake recovery shown by the recovery of VGAT expression, IPSC frequency is also reduced. As a result, vasopressin neuronal activity recovered from tonic inhibition. These possibilities remain to be investigated in order to link effects of hypoosmotic challenge on vasopressin neuronal activity to extracellular β-alanine levels and changes in β-alanine release from astrocytes. However, the present results clearly support that there is a coordinated modulation of astrocytes with neurones in the GABAergic inhibition.

Contribution of GFAP to astrocytic neuronal interactions during hypoosmotic challenge

GFAP plays a critical role in astrocytic plasticity (Wang & Hamilton, 2009). In the present study, we identified that hypoosmotic stimulation could elicit transient increase in GFAP expression. The early increases in GFAP are in agreement with hypoosmolality-elicited astrocyte swelling and expansion of astrocyte processes (Wilhelmsson *et al.*, 2004). Expanded astrocytic processes can reduce vasopressin neuronal activity by increasing glutamate and K^+ absorption, decreasing glutamatergic innervations, junctional communication and interactions between neighbouring vasopressin neurones (Hatton, 2004; Theodosis *et al.*, 2008). Longer hypoosmotic stimulation reversibly reduced GFAP levels, which could underlie retraction of astrocytic processes (Wang & Hatton, 2009), thereby promoting vasopressin release (Hatton, 2004; Theodosis *et al.*, 2008). In this study, we further identified a molecular association between GFAP and VGAT and this association changes correlatively with the alteration of firing activity of vasopressin neurones. The physical interaction between GFAP and VGAT, together with the association of GFAP with other astrocyte molecules such as actin, aquaporin-4, glutamine synthetase and serine racemase (Wang & Hatton, 2009), indicates that GFAP does not only interact with intermediate filaments (e.g. vimentine, nestine, and GFAP itself), it also interacts with other astrocytic proteins. Thus, this result supports our view that GFAP functions more than a structural protein (Wang & Hamilton, 2009). Together with previous findings, the present results indicate that GFAP functions in anchoring astrocytic proteins, including VGAT.

Conclusions

This work shows that in response to hypoosmotic challenge, vasopressin neurone firing is transiently reduced by GABAergic inhibition through synergistic interactions between astrocytes and SON neurones. Additional studies are needed to understand the full extent of neuronal-glial interactions that regulate hydromineral balance such as hyponatraemia-associated hypersecretion of vasopressin (Verbalis, 2010; Wang *et al.*, 2011).

Acknowledgments

We thank late Dr. Glenn I. Hatton for supervising this work initially. We thank Drs. John A. Russell and Todd A. Ponzio for advice, Harold Gainer for PS41 antibody. Research was sponsored by NIH grants NS009140 (University of California, Riverside) and DC007876 (LSU Health Sciences Center, Shreveport).

Abbreviations

GATs	GABA transporters
GFAP	glial fibrillary acidic protein
haCSF	hypoosmotic artificial CSF
naCSF	normal artificial CSF
L-AAA	l-aminoadipic acid
PVDF	polyvinylidene difluoride
RVD	regulatory volume decrease
SON	supraoptic nucleus
VGAT	Vesicular GABA transporter
VP-NP	vasopressin-neurophysin

References

Armstrong WE, Stern JE. Electrophysiological and morphological characteristics of neurons in perinuclear zone of supraoptic nucleus. J Neurophysiol. 1997; 78:2427–2437. [PubMed: 9356394]

Brown CH, Bull PM, Bourque CW. Phasic bursts in rat magnocellular neurosecretory cells are not intrinsically regenerative in vivo. Eur J Neurosci. 2004; 19:2977–2983. [PubMed: 15182304]

Bull PM, Brown CH, Russell JA, Ludwig M. Activity-dependent feedback modulation of spike patterning of supraoptic nucleus neurons by endogenous adenosine. Am J Physiol Regul Integr Comp Physiol. 2006; 291:R83–R90. [PubMed: 16497815]

Caldwell HK, Lee HJ, Macbeth AH, Young WS 3rd. Vasopressin: Behavioral roles of an "original" neuropeptide. Prog Neurobiol. 2007

Colombo JA. Glutamate uptake by rat brain astroglia incubated in human cerebrospinal fluid. Med Sci Monit. 2005; 11:BR13–BR17. [PubMed: 15614184]

Crowley WR, Armstrong WE. Neurochemical regulation of oxytocin secretion in lactation. Endocr Rev. 1992; 13:33–65. [PubMed: 1348224]

Cui LN, Saeb-Parsy K, Dyball RE. Neurones in the supraoptic nucleus of the rat are regulated by a projection from the suprachiasmatic nucleus. J Physiol. 1997; 502(Pt 1):149–159. [PubMed: 9234203]

Gainer H, Sarne Y, Brownstein MJ. Biosynthesis and axonal transport of rat neurohypophysial proteins and peptides. J Cell Biol. 1977; 73:366–381. [PubMed: 858741]

Ghavanini AA, Mathers DA, Kim HS, Puil E. Distinctive glycinergic currents with fast and slow kinetics in thalamus. J Neurophysiol. 2006; 95:3438–3448. [PubMed: 16554506]

Haam J, Popescu IR, Morton LA, Halmos KC, Teruyama R, Ueta Y, Tasker JG. GABA is excitatory in adult vasopressinergic neuroendocrine cells. J Neurosci. 2012; 32:572–582. [PubMed: 22238092]

Hatton GI. Dynamic neuronal-glial interactions: an overview 20 years later. Peptides. 2004; 25:403–411. [PubMed: 15134863]

Honda K, Negoro H, Higuchi T, Tadokoro Y. The role of the anteroventral 3rd ventricle area in the osmotic control of paraventricular neurosecretory cells. Exp Brain Res. 1989; 76:497–502. [PubMed: 2792243]

Hussy N, Deleuze C, Desarmenien MG, Moos FC. Osmotic regulation of neuronal activity: a new role for taurine and glial cells in a hypothalamic neuroendocrine structure. Prog Neurobiol. 2000; 62:113–134. [PubMed: 10828380]

Hussy N, Deleuze C, Pantaloni A, Desarmenien MG, Moos F. Agonist action of taurine on glycine receptors in rat supraoptic magnocellular neurones: possible role in osmoregulation. J Physiol. 1997; 502(Pt 3):609–621. [PubMed: 9279812]

Israel JM, Poulain DA, Oliet SH. Glutamatergic inputs contribute to phasic activity in vasopressin neurons. J Neurosci. 2010; 30:1221–1232. [PubMed: 20107050]

Kim JS, Kim WB, Kim YB, Lee Y, Kim YS, Shen FY, Lee SW, Park D, Choi HJ, Hur J, Park JJ, Han HC, Colwell CS, Cho YW, Kim YI. Chronic hyperosmotic stress converts GABAergic inhibition into excitation in vasopressin and oxytocin neurons in the rat. J Neurosci. 2011; 31:13312–13322. [PubMed: 21917814]

Kusano K, House SB, Gainer H. Effects of osmotic pressure and brain-derived neurotrophic factor on the survival of postnatal hypothalamic oxytocinergic and vasopressinergic neurons in dissociated cell culture. J Neuroendocrinol. 1999; 11:145–152. [PubMed: 10048470]

Lee S, Yoon BE, Berglund K, Oh SJ, Park H, Shin HS, Augustine GJ, Lee CJ. Channel-mediated tonic GABA release from glia. Science. 2010; 330:790–796. [PubMed: 20929730]

Leng G, Blackburn RE, Dyball RE, Russell JA. Role of anterior peri-third ventricular structures in the regulation of supraoptic neuronal activity and neurohypophysical hormone secretion in the rat. J Neuroendocrinol. 1989; 1:35–46. [PubMed: 19210480]

Ludwig M, Leng G. GABAergic projection from the arcuate nucleus to the supraoptic nucleus in the rat. Neurosci Lett. 2000; 281:195–197. [PubMed: 10704776]

Miyata S, Matsushima O, Hatton GI. Taurine in rat posterior pituitary: localization in astrocytes and selective release by hypoosmotic stimulation. J Comp Neurol. 1997; 381:513–523. [PubMed: 9136807]

Muller W, Hallermann S, Swandulla D. Opioidergic modulation of voltage-activated K+ currents in magnocellular neurons of the supraoptic nucleus in rat. J Neurophysiol. 1999; 81:1617–1625. [PubMed: 10200198]

Park JB, Jo JY, Zheng H, Patel KP, Stern JE. Regulation of tonic GABA inhibitory function, presympathetic neuronal activity and sympathetic outflow from the paraventricular nucleus by astroglial GABA transporters. J Physiol. 2009; 587:4645–4660. [PubMed: 19703969]

Park JB, Skalska S, Stern JE. Characterization of a novel tonic gamma-aminobutyric acidA receptor-mediated inhibition in magnocellular neurosecretory neurons and its modulation by glia. Endocrinology. 2006; 147:3746–3760. [PubMed: 16675519]

Pasantes-Morales H, Alavez S, Sanchez Olea R, Moran J. Contribution of organic and inorganic osmolytes to volume regulation in rat brain cells in culture. Neurochem Res. 1993; 18:445–452. [PubMed: 8097294]

Pasantes-Morales H, Vazquez-Juarez E. Transporters and Channels in Cytotoxic Astrocyte Swelling. Neurochem Res. 2012

Paterson JA, Leblond CP. Increased proliferation of neuroglia and endothelial cells in the supraoptic nucleus and hypophysial neural lobe of young rats drinking hypertonic sodium chloride solution. J Comp Neurol. 1977; 175:373–390. [PubMed: 915032]

Ponzio TA, Ni Y, Montana V, Parpura V, Hatton GI. Vesicular glutamate transporter expression in supraoptic neurones suggests a glutamatergic phenotype. J Neuroendocrinol. 2006; 18:253–265. [PubMed: 16503920]

Randle JC, Day TA, Jhamandas JH, Bourque CW, Renaud LP. Neuropharmacology of supraoptic nucleus neurons: norepinephrine and gamma-aminobutyric acid receptors. Fed Proc. 1986; 45:2312–2317. [PubMed: 3015685]

Richard D, Bourque CW. Synaptic control of rat supraoptic neurones during osmotic stimulation of the organum vasculosum lamina terminalis in vitro. J Physiol. 1995; 489(Pt 2):567–577. [PubMed: 8847648]

Shibuya I, Kabashima N, Ibrahim N, Setiadji SV, Ueta Y, Yamashita H. Pre- and postsynaptic modulation of the electrical activity of rat supraoptic neurones. Exp Physiol. 2000; 85(Spec No): 145S–151S. [PubMed: 10795917]

Sladek CD, Armstrong WE. gamma-Aminobutyric acid antagonists stimulate vasopressin release from organ-cultured hypothalamo-neurohypophyseal explants. Endocrinology. 1987; 120:1576–1580. [PubMed: 2435537]

Theodosis DT, Poulain DA, Oliet SH. Activity-dependent structural and functional plasticity of astrocyte-neuron interactions. Physiol Rev. 2008; 88:983–1008. [PubMed: 18626065]

Verbalis JG. Brain volume regulation in response to changes in osmolality. Neuroscience. 2010; 168:862–870. [PubMed: 20417691]

Voisin DL, Chapman C, Poulain DA, Herbison AE. Extracellular GABA concentrations in rat supraoptic nucleus during lactation and following haemodynamic changes: an in vivo microdialysis study. Neuroscience. 1994; 63:547–558. [PubMed: 7891864]

Wang Y-F, Hamilton K. Chronic vs. acute interactions between supraoptic oxytocin neurons and astrocytes during lactation: role of glial fibrillary acidic protein plasticity. ScientificWorldJournal. 2009; 9:1308–1320. [PubMed: 19936568]

Wang Y-F, Hatton GI. Interaction of Extracellular Signal-Regulated Protein Kinase 1/2 with Actin Cytoskeleton in Supraoptic Oxytocin Neurons and Astrocytes: Role in Burst Firing. Journal of Neuroscience. 2007; 27:13822–13834. [PubMed: 18077694]

Wang Y-F, Liu L-X, Yang H-P. Neurophysiological involvement in hypervolemic hyponatremia-evoked by hypersecretion of vasopressin. Translational Biomedicine. 2011; 2:2.

Wang YF, Hatton GI. Milk ejection burst-like electrical activity evoked in supraoptic oxytocin neurons in slices from lactating rats. J Neurophysiol. 2004; 91:2312–2321. [PubMed: 14724260]

Wang YF, Hatton GI. Astrocytic plasticity and patterned oxytocin neuronal activity: dynamic interactions. J Neurosci. 2009; 29:1743–1754. [PubMed: 19211881]

Wilhelmsson U, Li L, Pekna M, Berthold CH, Blom S, Eliasson C, Renner O, Bushong E, Ellisman M, Morgan TE, Pekny M. Absence of glial fibrillary acidic protein and vimentin prevents hypertrophy of astrocytic processes and improves post-traumatic regeneration. J Neurosci. 2004; 24:5016–5021. [PubMed: 15163694]

Yagil C, Sladek CD. Osmotic regulation of vasopressin and oxytocin release is rate sensitive in hypothalamoneurohypophysial explants. Am J Physiol. 1990; 258:R492–R500. [PubMed: 2309938]

Zhang B, Glasgow E, Murase T, Verbalis JG, Gainer H. Chronic hypoosmolality induces a selective decrease in magnocellular neurone soma and nuclear size in the rat hypothalamic supraoptic nucleus. J Neuroendocrinol. 2001; 13:29–36. [PubMed: 11123513]

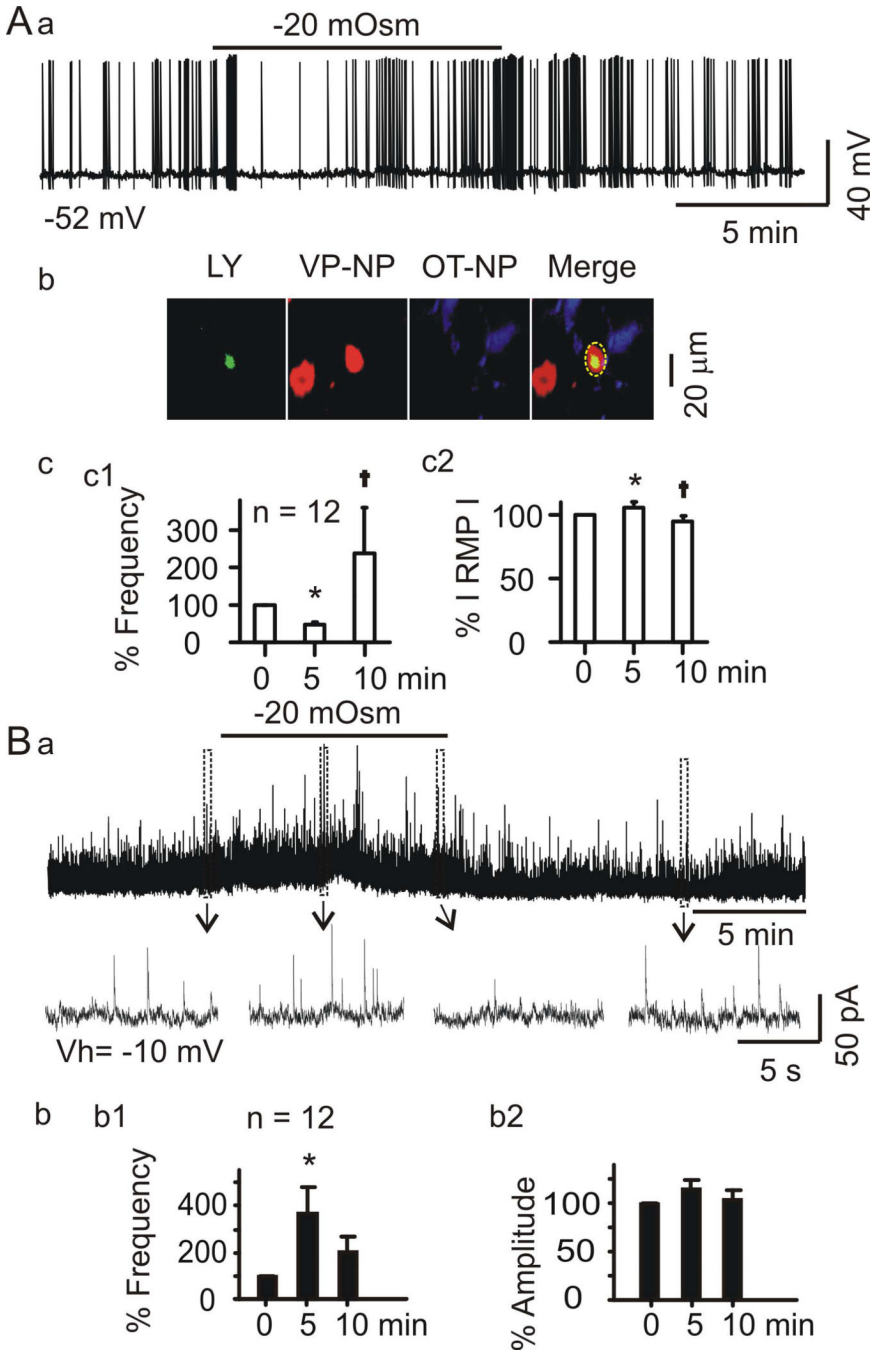

Figure 1.

Hypoosmotic challenge of rat brain slices decreases then restores firing rate and evokes correlated changes in inhibitory postsynaptic current (IPSC) frequency of vasopressin neurones in the SON. ***A***, Whole cell patch clamp recordings from vasopressin neurones. ***Aa***, Firing activity of a phasically-firing neurone in normal aCSF (305 mOsm, naCSF) before and after superfusing the slice with −20 mOsm hypoosmotic aCSF (haCSF). Number at bottom left indicates initial membrane potential. ***Ab***, Post hoc immunostaining of recorded supraoptic neurones. Confocal microscopic images (63× objective) of the recorded cells, which were filled with Lucifer yellow (LY) and showed immunoreactivity for vasopressin-neurophysin (VP-NP), but not for oxytocin neurophysin (OT-NP). The dashed circle in

merged channel points to the overlapping of LY and VP-NP staining. ***Ac***, Mean (± SEM) changes (%) in firing rate (***Ac1***) and absolute value of the membrane potential (RMP, ***Ac2***) after 5 and 10 min superfusion with haCSF, relative to naCSF (0 min in haCSF). In all figures, $*P<0.05$ vs. 0 min and $\dagger P<0.05$ compared to 5 min by ANOVA. ***B***. IPSC (***Ba***) recorded from a neurone at −10 mV. Regions indicated by boxes are expanded below the traces. ***Bb1***, Mean ± SEM changes (%) in IPSC frequency after 5 and 10 superfusion of haCSF relative to 0 min.

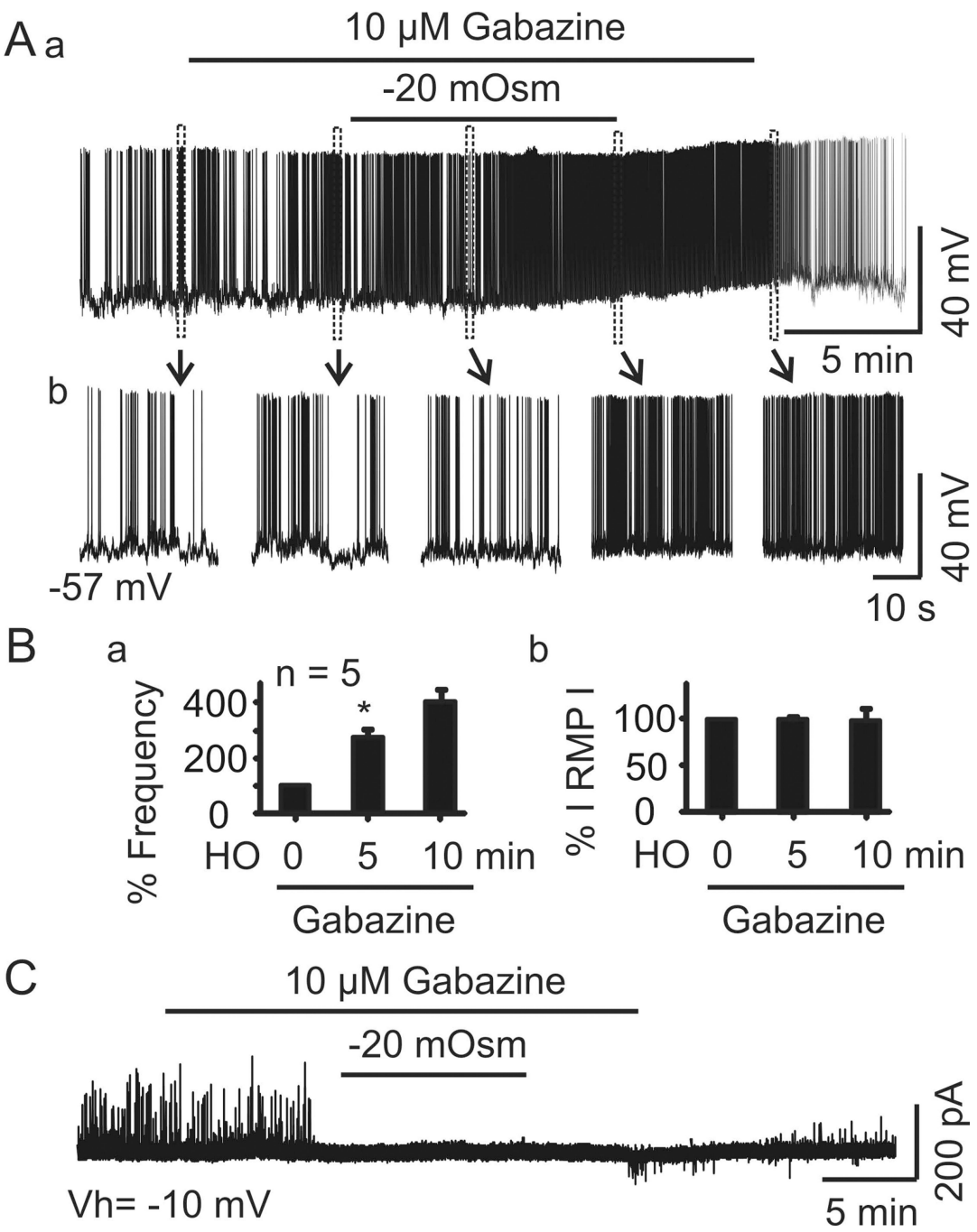

Figure 2.

$GABA_A$ receptor-mediated IPSCs are inhibitory in vasopressin neurones. ***A***, current-clamp recordings of firing activity of a putative vasopressin neurone in the presence of gabazine (10 μM) in naCSF and then with gabazine in haCSF. Boxes in ***Aa*** indicate regions expanded in ***Ab***. ***B***, Changes in mean ± SEM firing frequency (%, ***Ba***) and absolute value of the membrane potential (%, ***Bb***) after 5 and 10 min superfusion with haCSF containing gabazine, relative to 0 min. ***C***, Representative trace in voltage-clamp recording of IPSCs in the presence of gabazine at −10 mV.

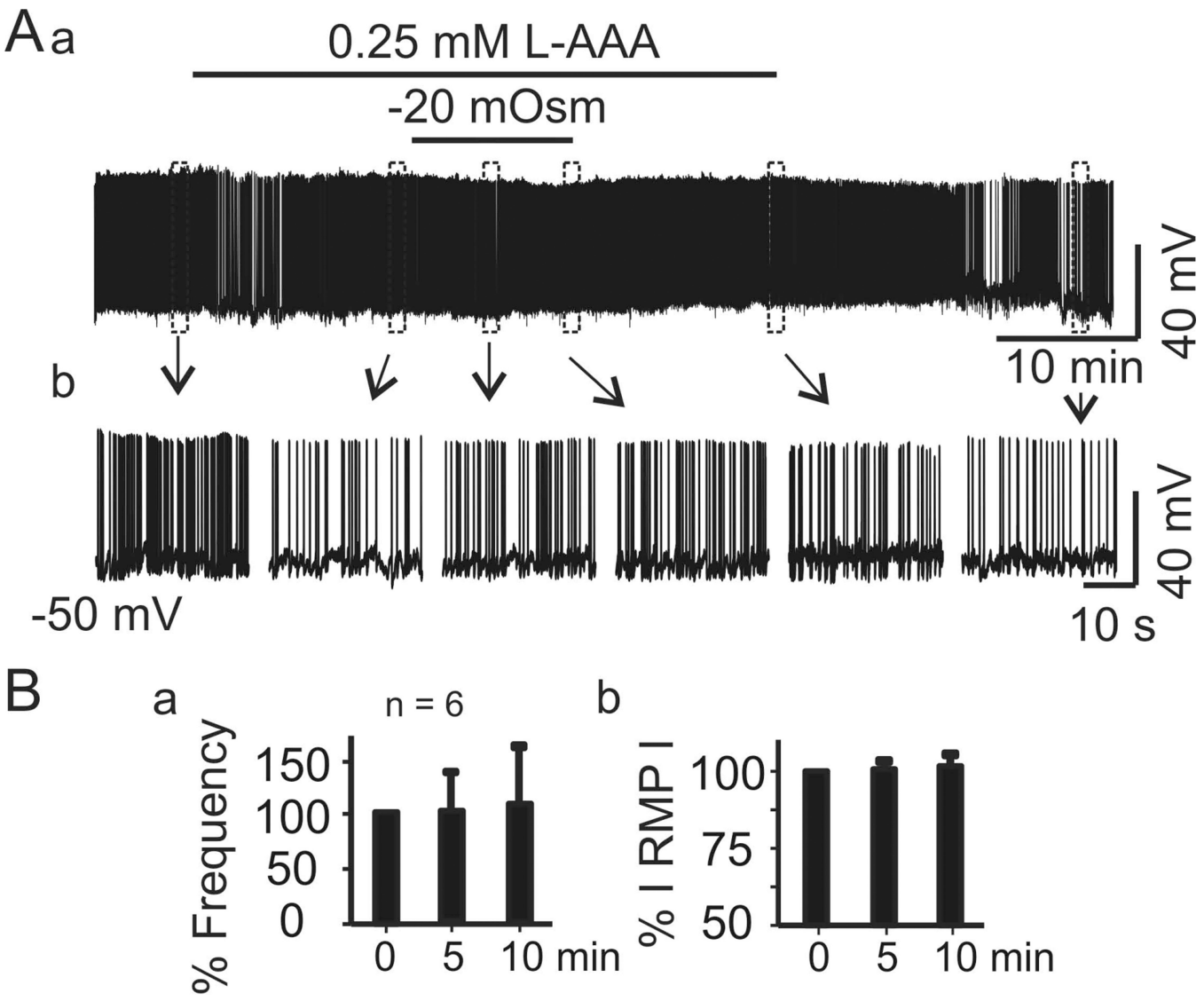

Figure 3.

Disruption of astrocyte functions blocks hypoosmotic suppression or later recovery of vasopressin neurone firing. ***A***, Firing activity of a vasopressin neurone in naCSF containing the gliotoxin l-aminoadipic acid (L-AAA, 0.25 mM) before and after superfusion with haCSF containing L-AAA, in full recording (***Aa***) and expanded episodes (***Ab***). ***B***, Mean ± SEM changes (%) in firing rate (***Ba***) and absolute value of the membrane potential (RMP, ***Bb***) of 6 cells after 5 and 10 min superfusion, relative to 0 min. No significant differences were observed.

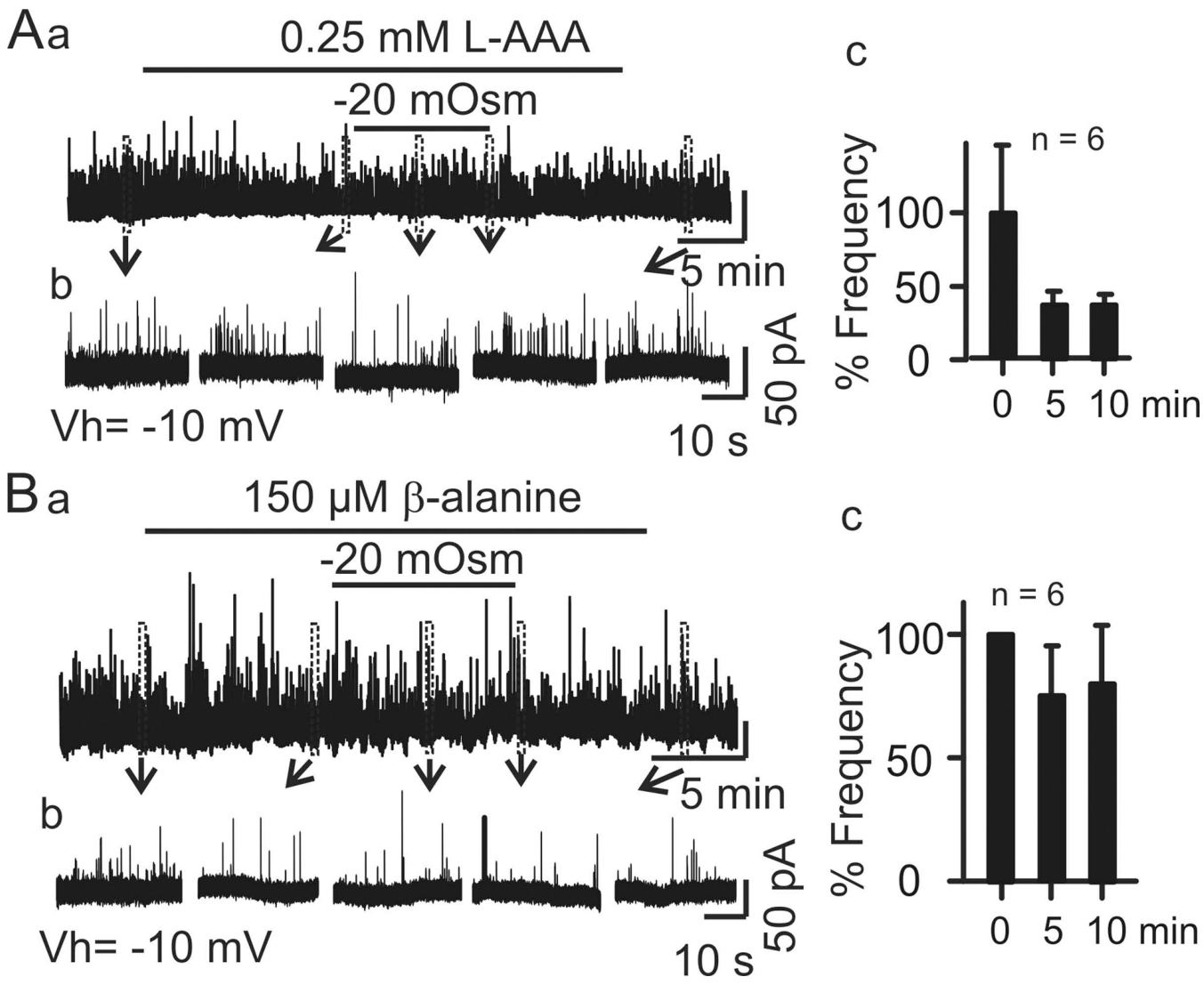

Figure 4.

Blocking astrocytic GABA transport reduces effects of hypoosmotic challenge on IPSC frequency. ***Aa–c***, Effects of superfusion with L-AAA in haCSF on IPSC frequency, relative to 0 min. ***Ba–c***, Effects of superfusion with β-alanine (0.15 mM) in haCSF on IPSC frequency, relative to 0 min.

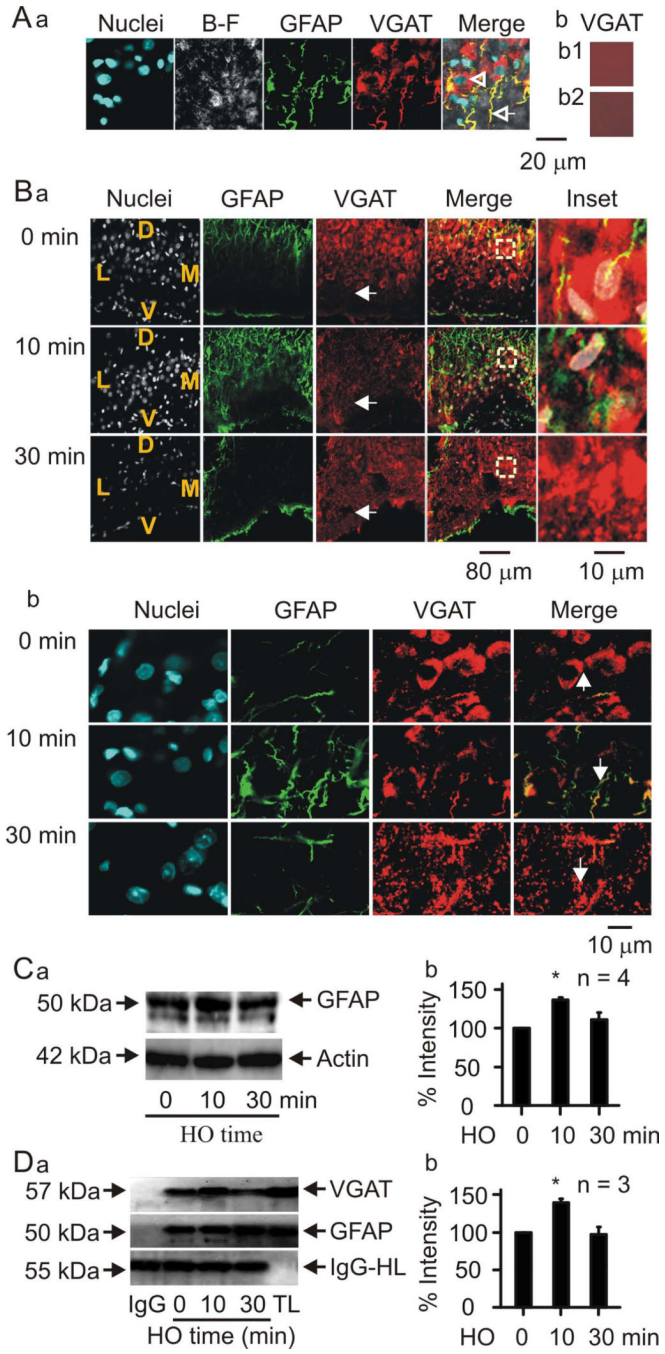

Figure 5.

Hypoosmotic challenge modulates expression of vesicular GABA transporter (VGAT) in both astrocytes and neurones of the SON. ***A***, Confocal microscopic images of the SON in a hypothalamus slice. ***Aa***, Representative images showing (from left to right) nuclei, bright-field (B–F) view of the slice, GFAP, VGAT and the merged view. The open arrowhead indicates a neuronal nucleus and the open arrow points to an astrocytic process. ***Ab1*** and ***Ab2***, Negative controls in the presence of goat antibody against VGAT without secondary antibody (*Ab1*) and Alexa Fluor 555-labelled secondary antibody without primary antibody (*Ab2*), respectively. ***B***, Time-dependent effects of *in vivo* hypoosmotic challenge on GFAP and VGAT expression. ***Ba***, Representative confocal images (from left to the right) showing

staining of nuclei, GFAP, VGAT, their merges and the expanded insets (from the squared areas in the merged channel), respectively. From top to the bottom, the panels showing times at 0 min (immediately), 10 min and 30 min of after i.p. application of hypoosmotic solution (20 ml/kg, i.p.). The letters in the nuclei channels show the orientation of the SON in the slices: V, ventral; D, dorsal; M, medial; L, lateral side. White arrows indicate the VGAT staining in the ventral glial lamina (bottom). ***Bb***, Same images as ***Ba*** but in higher amplification. ***Bc***, Summary graphs showing the general change in VGAT intensity (left) and the number of VGAT-positive somata of magnocellular neurones (right). ***C***, Effects of *in vivo* hypoosmotic challenge on GFAP levels. Left panels (***Ca***) show Western blot bands and the bar graph (***Cb***) summarises quantitative data expressed as percentage of control GFAP level relative to actin (loading control). ***D***, co-immunoprecipitation of GFAP with VGAT after 0, 10 and 30 minutes of *in vivo* hypoosmotic challenge. IgG-HC, IgG heavy chain, used as negative control; TL, total lysates, used as positive control.